ELECTROMECHANICAL, ACOUSTICAL, AND THERMAL CHARACTERIZATION OF PIEZOCERAMIC ELEMENTS AT DIFFERENT DRIVING CONDITIONS

Petar Franček, Antonio Petošić, Marko Horvat, Marko Budimir

Department of Electroacoustics, Faculty of Electrical Engineering and Computing, University of Zagreb, Unska 3, 10000 Zagreb, Croatia
Institute for Nuclear Technology, Unska 3, 10000 Zagreb, Croatia

Abstract: The results of electromechanical characterization made on piezoceramic elements are not consistent when standardized methods are used to determine the values of material parameters. When a given method is used for such a characterization, the results will depend on the excitation level and temperature. Applying excitations with different signal magnitudes (voltage, current and applied electrical power), the output characterization results (displacement, sound pressure, temperature) confirms aforementioned thesis. This paper compares the results of a method with fast frequency sweeps for full electromechanical and acoustical characterization of hard, soft, and lead-free piezoceramic bulk elements at low (1 V_{RMS}) and high excitation levels (up to 20 V_{RMS}) at series resonance. The temperature is tracked during measurements and the results show significant difference between the values of measured parameters (resonance frequency, electrical admittance, displacement, and pressure magnitudes changes) obtained with different measurement methods, with nonlinear and temperature effects (due to self-heating) coupled or treated separately.
The increase of the excitation signal magnitude from low (1 V_{RMS}) to high (20 V_{RMS}) in or near resonance leads to the decrease of the input electrical admittance magnitude of up to 90% due to coupled nonlinear and temperature change effects, and the decrease of the resonance frequency up to 2%, compared to low-level resonance frequency measured at room temperature.

Keywords: ultrasound, piezoceramic, electromechanical characterization, high voltage excitation

1. INTRODUCTION

The application of the piezoelectric effect has been known for more than a century and is rapidly increasing. The piezoelectric effect was discovered by the Curie brothers in 1880 [1, 2, 3], and the first notable application occurred in 1919 when a natural crystal, quartz, was used as an electrical oscillator [4]. The steady increase in applications was enhanced during World War II by the discovery of the piezoelectric effect in some man-made polycrystalline materials (ceramics) using the polarization process [3]. The result was cheap piezoceramics in any shape and with almost unlimited supply. Moreover, it was possible to adjust properties of the manufactured ceramics for a particular use by changing the ratio and type of doped substances. With the development of electronics in the second half of the last century, the commercial use of ultrasound devices increased. Sonography, a medical imaging used to confirm and monitor pregnancy, is probably the best known use of ultrasound, but there are numerous applications in a variety of fields.

The requirements for a modern device have evolved, leading to an additional expansion of possible applications. Nowadays, it is normal to have battery-powered wireless or mobile devices with a variety of functions. Portability is a specific request where many prerequisites need to be fulfilled. These devices must be small and light, have low power consumption, and have long battery life. Due to the different environmental conditions, the devices must be adaptable, efficient and safe to use in different conditions. Therefore, an ultrasonic system must have high efficiency, which can be achieved by exciting a piezoceramic transducer in resonance. Different types of piezoceramic elements (soft, hard and lead-free ceramics) are used in low and

high power ultrasonic transducers for various applications (Non-Destructive Testing (NDT), welding, cleaning, therapeutic, surgical and diagnostic ultrasound in medicine). The excitation frequency range of applied ultrasound is from 20 kHz to several hundred megahertz and even to the gigahertz range for some applications (the most common use of high frequency ultrasound is in acoustic microscopes - NDT, for research in biology) [5] with different types of signals (pulse, sine, etc.).

2. RESONANCE, NONLINEARITIES AND EQUIVALENT CIRCUITS

Excitation of a piezoceramic element in resonance results with a significant increase in gain compared to piezoceramics excited out of resonance. As a negative consequence, excitation in resonance has noticeable nonlinear effects leading to very high instability and unpredictability.

In the literature, there are few definitions of resonant (serial) and antiresonant (parallel) frequency [6]. In this paper, resonant (f_s) and antiresonant (f_p) frequencies are defined as frequencies where the excitation signal of current and voltage are in phase. Around these frequencies, there are extremes of electrical impedance, where the impedance minimum is defined as resonant frequency and the maximum is defined as antiresonant frequency. The resonant frequency is affected by nonlinearities that depend on the strength of the excitation, temperature, or pressure rise. The design of an ultrasound device that meets the requirements mentioned in the introduction is a comprehensive task.

2.1. Electrical equivalent circuit

The representation of a piezoelectric component in the electrical domain is well described in IEEE Standard on piezoelectricity, IEEE Std 176-1978 [7]. An electrical equivalent circuit (RLC) of a piezoelectric element described in this standard is shown in Fig. 1.

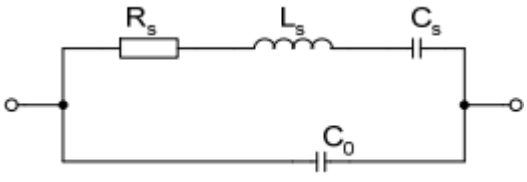

Fig.1. *RLC Equivalent Electrical Circuit of a Piezoelectric Vibrator [8]*

This is a commonly used equivalent for piezoceramic elements in electrical circuits. Among the numerous alternatives and improvements proposed, the Mason and KLM models are well known and are shown in Fig. 2 [9, 10].

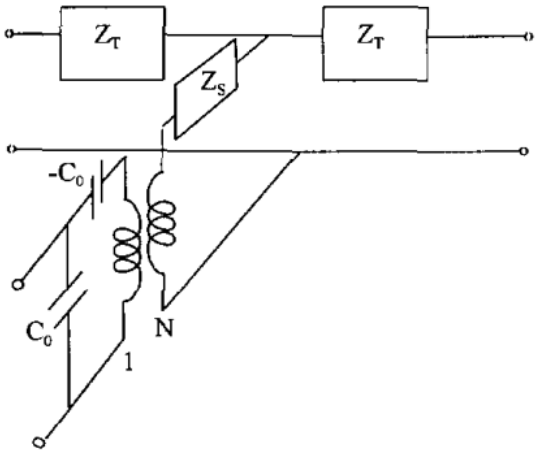

Fig.2. *KLM Equivalent Electrical Circuit of a Piezoelectric Vibrator*

KLM and Mason equivalent circuits are more complex due to the additional front and rear vibrating masses. The advantage of this model over the standard RLC model is that mechanical signals can be calculated on the surface of a assembled transducer as well as for components of the transducer [11, 12].

According to the nomenclature in Fig. 1, the impedance (*Z*) of a circuit can be expressed as the reciprocal of the admittance (*Y*):

$$Y = \frac{1}{Z} = \frac{1}{R_0} + j\omega C_0 + \frac{1}{R_S + j\omega L_S + \frac{1}{j\omega C_S}} \qquad (1)$$

Assuming that there is no imaginary part of equation 1 in resonance, it is easy to determine the resonant frequencies of a piezoceramic. Equation 2 defines serial (f_s) and parallel (f_p) resonant frequencies:

$$f_s = \frac{1}{2 \cdot \pi} \cdot \sqrt{\frac{1}{L_S \cdot C_S}} \qquad f_p = \frac{1}{2 \cdot \pi} \cdot \sqrt{\frac{C_S + C_0}{L_S \cdot C_S}} \qquad (2)$$

By measuring the resonant frequency of a piezoelectric transducer, it is easy to calculate the resonant parameters for this model. The resistance R_0 and capacitance C_0 are determined far from the resonance, so the influence of an

electrical resonant branch on measured parameters is minimal.

2.2. Mechanical equivalent circuit

A simple mathematical oscillator with a spring is used for the mechanical representation of the ceramic transducer. Two masses (*m*) are coupled with a spring (with stiffness k^E) as shown in Fig. 3.

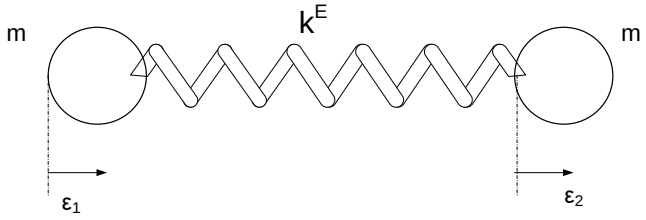

Fig.3. *Part of a piezoelectric element presented as a coupled mass oscillator*

The displacement (*d*) of an observed piezoelectric element is calculated as the difference of the displacement of each mass (ε_1 - ε_2) and *N* represents the piezoelectric force. When a force (F_1) is applied to a mass, the equation of motion for the first mass (left in Fig. 3) which is in the electric field (*U*), is given in the form 3 [13]:

$$m \cdot \varepsilon_1 = F_{spr} + F_1 = -k^E \cdot d + N \cdot U + F_1 \qquad (3)$$

The vibration of a piezoelectric element is in both directions, and because of the mirroring, it is easy to represent it as a 1D oscillation. Using complex parameters in equation 3, the full equation of motion including the real and imaginary parts of the mechanical impedance with added nonlinearities is obtained [13]:

$$\left[m + \frac{Im(Z_m)}{\omega}\right] \cdot \ddot{\varepsilon}_1 + [2 \cdot d_m + Re(Z_m)] \cdot \dot{\varepsilon}_1 + 2 \cdot k^E \cdot \varepsilon_1 = N \cdot U \qquad (4)$$

d_m stands for mechanical damping and $\ddot{\varepsilon}_1$ and $\dot{\varepsilon}_1$ for the first and second derivation of a displacement.
Using the same assumptions as for the electrical equivalent circuit, a resonant frequency can be derived:

$$f_s = \frac{1}{2 \cdot \pi} \cdot \sqrt{\frac{k^E}{m}} \qquad (5)$$

3. LABORATORY SETUP

The laboratory setup is designed to record measurement data from multiple sensors simultaneously with minimal time offset between different measurement signals. The Agilent MSO-3024A 200 MHz digital oscilloscope can measure up to 4 signals from the sensors. The sensors are located on a piezoceramic surface or connected to appropriate electrical wires. In the electrical domain, 2 signals are recorded on a ceramic, voltage with the Testec TT-SI 9001 probe (bandwidth 25 MHz, voltage up to 1400 V) and current with the Tektronix TCP312 probe (frequency range up to 100 MHz and level from mA to 30 A), whose signal is processed by a dedicated amplifier (Tektronix TCP 300). The displacement is measured with the photonic sensor MTI-2100 and the acoustic pressure with the Bruel&Kjaer miniature hydrophone type 8103 (frequency range up to 180 kHz) with its own B&K Nexus preamplifier. The excitation signals are generated using a 20MHz Keysight 33512b 2-channel arbitrary waveform generator. The output of the generator is connected to an E&I Power Amplifier 2100L with a declared electrical input impedance of 50 Ω and an output impedance of 50 Ω, which was further verified by measuring voltage and current across the calibrated electrical loads. The power amplifier is connected to the ceramic via a 0.5 m coaxial cable (50 Ω characteristic impedance). A computer with a Matlab controled algorithm is the centre of the setup. Fig. 4 shows a laboratory setup with all five sensors.

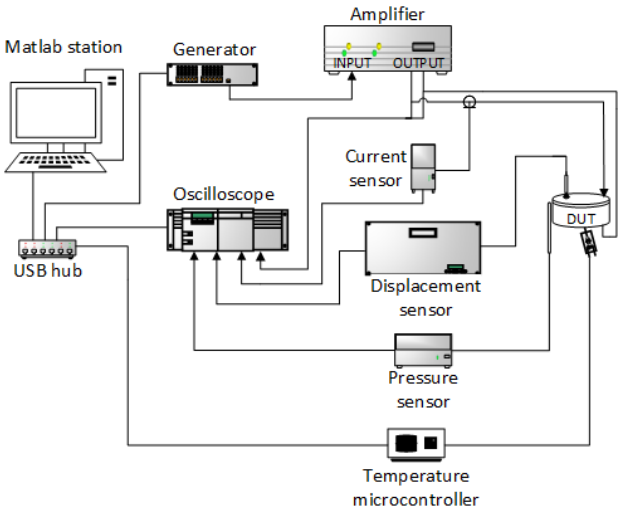

Fig.4. *Laboratory setup*

A device with NodeMCU microcontroller has been developed for temperature measurements. It is powered through USB port and contactless infrared thermometer MLX90614 is used as sensor. The sensors are contactless so that their influence is minimized during the measurement process. To achieve thermal characterization, the samples with the sensors are positioned in an oven with a temperature control of ±1 ℃. Measurements are performed at three different temperatures, 25 ℃, 50 ℃ and 75℃.

Special Matlab methods are used to control the laboratory devices. The excitation signals are controlled by a generator, and the information from the sensors is collected by specific commands with an oscilloscope and a temperature sensor. Matlab is a convenient programming language with functional diversity, excellent hardware and software support, and a strong community. After collecting the data, it is possible to process, store or even display it in real time. It is easy to process the data using the built-in mathematical methods, preview it, or transform it in any way. For the purpose of additional and thorough data manipulation, records are stored in a predefined database.

4. MEASUREMENT RESULTS

Four piezoceramic bulk samples are used for the measurements. These four samples are manufactured in specialized factories so that the piezoceramic parameters can be defined and confirmed. The measurements are performed with impedance spectrography in frequency range of interest with voltage levels from 1 V to 20 V. All piezoceramic samples have a similar diameter, so the measurements are performed in radial oscillation mode (30 - 80 kHz). Some physical properties of the measured samples are listed in Table 1.

Sample Name	Mass [g]	Diameter [mm]	Thickness [mm]
APC50	150	49.2	10.1
PiHard	76	50	5
PiSoft	76	50	5
Pi700	54	50.9	4.7

Table 1. *Mass, diameter, and thickness of a measured samples*

The APC50 piezoceramic is twice as thick as other ceramics, but because of the minimal difference in diameter, this difference is easily negligible when measurements are made in the radial mode.

To confirm the results of the measurements, three different types of piezoceramics are used. Hard piezoceramic samples are APC50 and PiHard. Soft piezoceramic is PiSoft and the lead-free ceramic Pi700, which is very popular today. APC50 is from the manufacturer American Piezo Ceramics (USA), and others are from the manufacturer PiCeramic (Germany).

The frequency range of measurements is set individually for each ceramic sample. Fig. 5 shows the results for an APC50 sample.

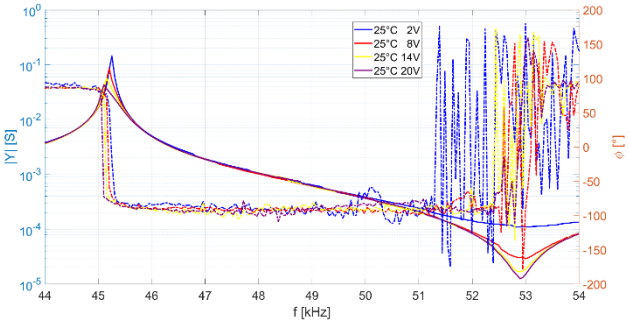

Fig.5. *Admittance and phase of a APC50 sample on a temperature T = 25 ℃*

It is important to note that the vertical axis is the admittance (*Y*), so the graph is inverted compared to the impedance graph. In Fig. 5 it is shown how the admittance parameter depends on the level of excitation. Also, in the same figure the angle (ϕ) between current and voltage excitation signals is shown. It is easy to see that the extremes of the admittance (impedance) are at the frequency points where current and voltage signals are in phase.

4.1. APC50 sample results

At the beginning of the results preview, the most representative ceramic is displayed, an APC50. In the first figures the measurements for temperature T=25 ℃ are displayed. Three figures show respectively a plot of impedance, pressure and displacement, as shown in figures Fig. 6, Fig. 7 and Fig. 8.

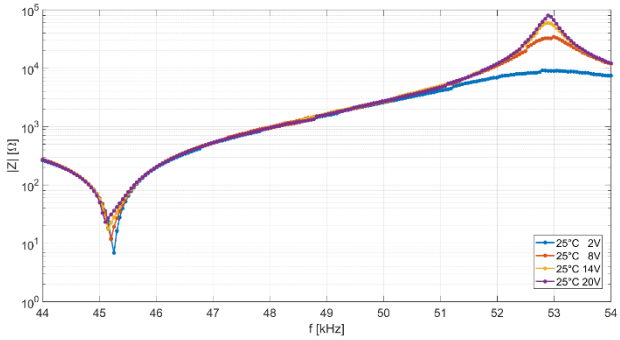

Fig.6. *Impedance magnitude of a APC50 sample (T=25 ℃)*

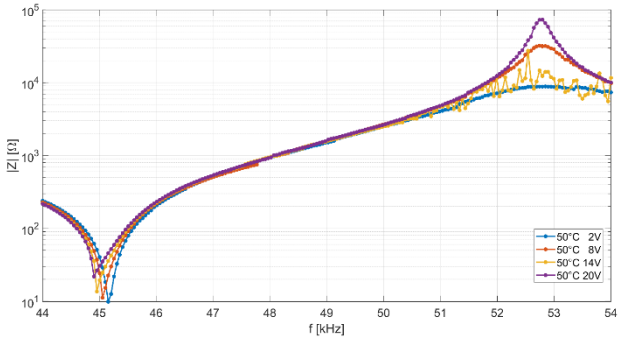

Fig.9. *Impedance magnitude of a APC50 sample (T=50 ℃)*

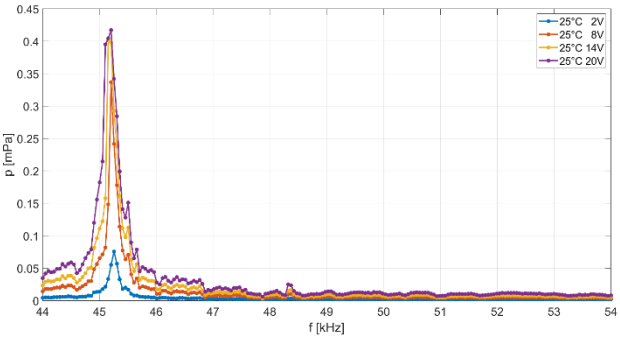

Fig.7. *Pressure of a APC50 sample (T=25 ℃)*

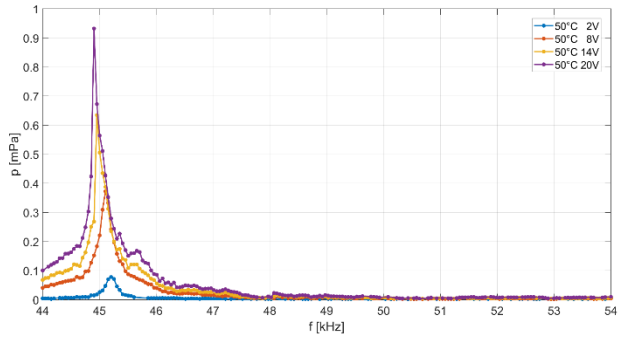

Fig.10. *Pressure of a APC50 sample (T=50 ℃)*

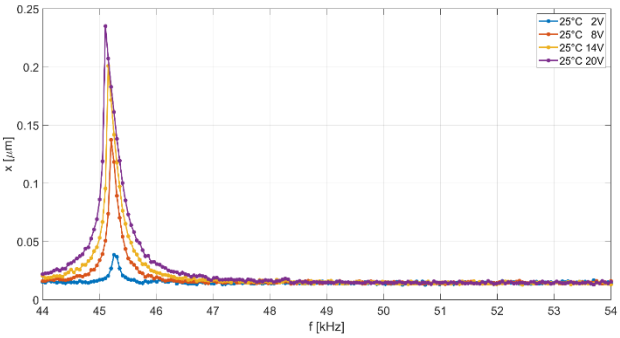

Fig.8. *Displacement of a APC50 sample (T=25 ℃)*

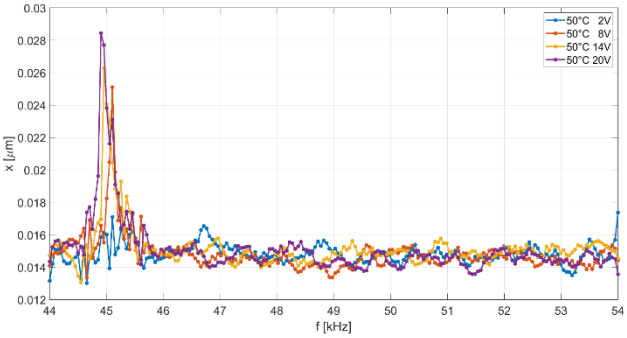

Fig.11. *Displacement of a APC50 sample (T=50 ℃)*

The above figures show that the resonant frequency decreases as the magnitude of the excitation increases. The magnitude of the impedance increases, and the same is true for the pressure and displacement.

The results of the measurements carried out at a temperature of T=50 ℃ on the same sample are shown in figures Fig. 9, Fig. 10 and Fig. 11 (impedance, pressure and displacement, respectively).

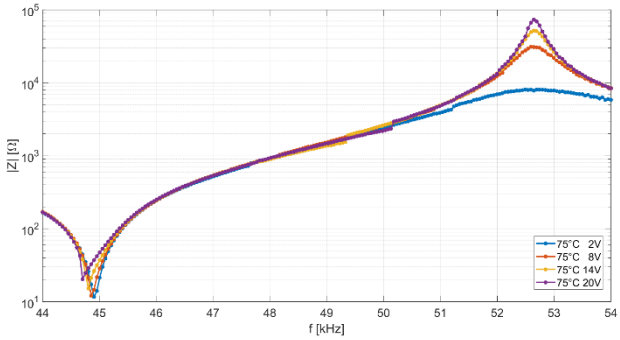

Fig.12. *Impedance magnitude of a APC50 sample (T=75 ℃)*

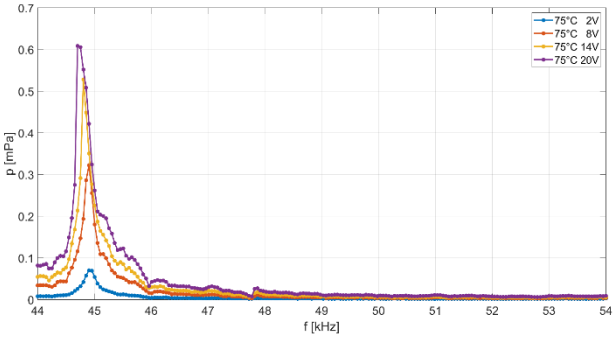

Fig.13. *Pressure of a APC50 sample (T=75 ℃)*

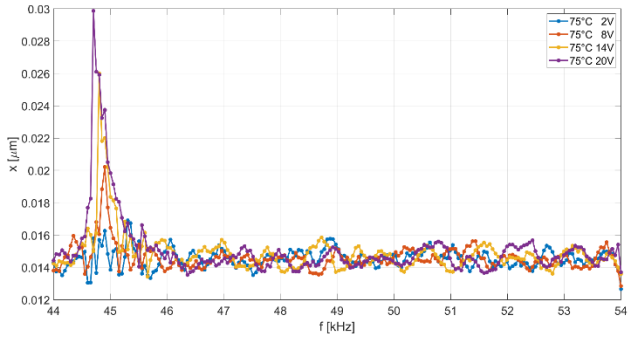

Fig.14. *Displacement of a APC50 sample (T=75 ℃)*

It is noticeable that the results are as expected: As the excitation level increases, the resonant frequency decreases, while impedance magnitude, pressure and displacement increase.

For the highest temperature (T=75 ℃), another set of three figures is shown (Fig. 12, Fig. 13, and Fig. 14). The results are shown in the same order as before, maintaining the same trend as the results for lower temperatures.

It is important to observe a voltage drop at the point of resonance, as shown in Fig. 15.

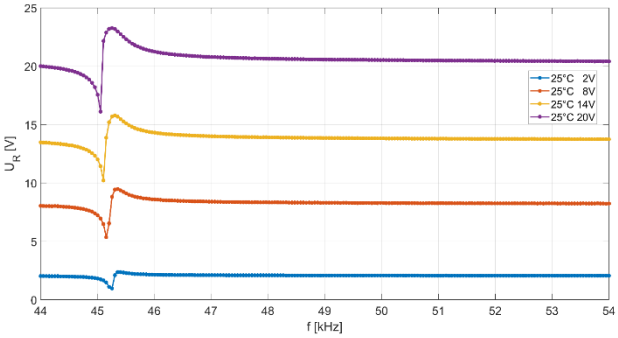

Fig.15. *Voltage drops in resonance on a APC50 sample*

This is the result of an impedance mismatch at resonance of a piezoceramic and excitation. This effect is present in all measurements conducted in this work.

A more convenient tabulated presentation is given for these and other samples. Table 2 shows the results for this sample.

U_{Exc} [V]	f_s [kHz]	$\|Z\|$ [Ω]	p [mPa]	x [μm]	U_R [V]	I_R [A]	P_R [W]
2	45.26	6.9	0.1	0.04	0.96	0.14	0.13
8	45.21	11.7	0.3	0.14	1.11	0.09	0.05
4	45.16	17.5	0.4	0.20	1.47	0.06	0.02
20	45.11	23.1	0.4	0.24	1.65	0.05	0.02
2	45.11	9.5	0.1	0.02	1.01	0.11	0.10
8	45.06	11.2	0.4	0.03	1.33	0.08	0.05
14	44.95	13.6	0.6	0.03	1.71	0.04	0.02
20	44.90	21.8	0.9	0.03	1.80	0.04	0.01
2	44.90	11.7	0.1	0.02	1.11	0.10	0.10
8	44.85	12.1	0.3	0.02	1.27	0.07	0.06
14	44.80	15.2	0.5	0.03	1.47	0.06	0.04
20	44.70	20.3	0.6	0.03	1.70	0.04	0.02

Table 2. *Measurement results of a APC50 ceramic*

Table 2 shows the results of the APC50 samples for three different temperatures. Green coloured rows are for 25 ℃, yellow for 50 ℃, and blue for 75 ℃. The first column of the table shows an excitation voltage U_{Exc}. This is an excitation level set by an algorithm. The other parameters listed are parameters measured during excitation at resonance, where f_S is the frequency of excitation, $|Z|$ is the magnitude of impedance, p is pressure, x is displacement, and U_R, I_R, and P_R are voltage, current, and power, respectively, measured directly on a sample.

4.2. PiHard sample results

The results of this and the following samples are shown primarily in tables. There is no need to clutter the paper with illustrations of results having the same

tendency. Only representative graphs are shown, and the detailed data is given in tables.

The results of impedance spectroscopy for temperature T=25 ℃ are shown in Fig. 16:

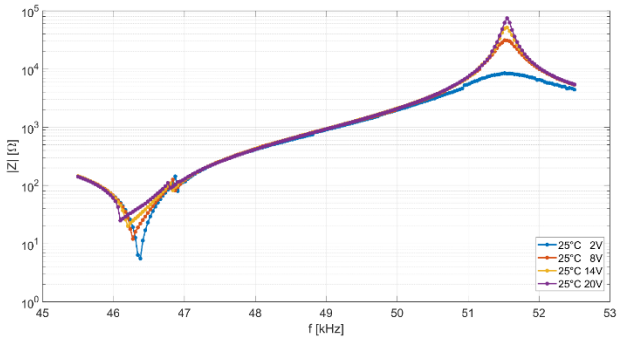

Fig.16. *Impedance magnitude of a PiHard sample (T=25 ℃)*

The measured pressure and displacement change according to changes in an impedance magnitude. Fig. 17 shows the results of a measured pressure and Fig. 18 that of a displacement.

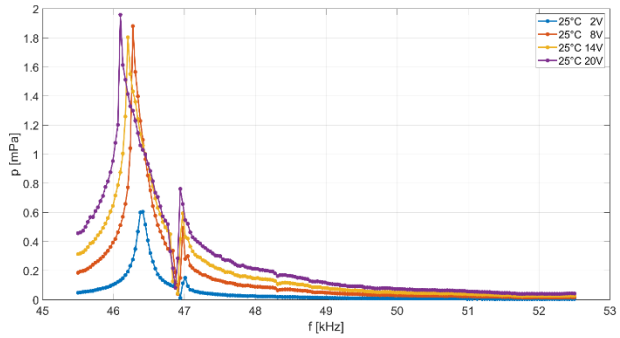

Fig.17. *Pressure of a PiHard sample (T=25 ℃)*

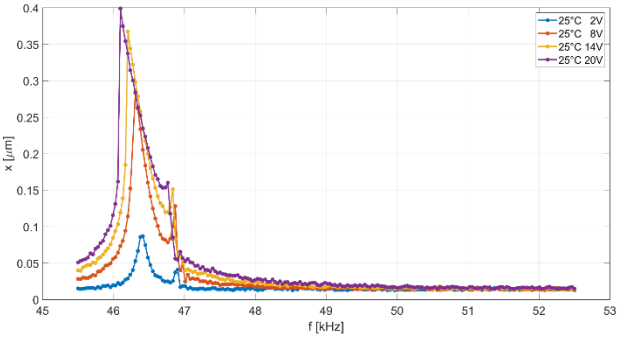

Fig.18. *Displacement of a PiHard sample (T=25 ℃)*

Table 3 contains the results of a PiHard ceramic measured near a resonance point. In this and the following tables, the convention of Table 2 is used. The order and abbreviations of the parameters listed are the same, and the results measured at different temperatures have the same colour coding as in Table 2.

U_{Exc} [V]	f_s [kHz]	|Z| [Ω]	p [mPa]	x [μm]	U_R [V]	I_R [A]	P_R [W]
2	46.38	5.5	0.6	0.09	0.92	0.17	0.13
8	46.27	12.1	1.9	0.28	1.48	0.08	0.03
14	46.20	20.1	1.8	0.37	1.73	0.05	0.01
20	46.10	24.8	2.0	0.40	1.89	0.04	0.01
2	46.45	6.4	0.6	0.06	0.80	0.12	0.08
8	46.34	10.6	1.9	0.21	1.53	0.06	0.02
14	46.27	20.5	2.3	0.28	1.69	0.05	0.01
20	46.17	25.5	2.9	0.35	1.82	0.03	0.01
2	46.59	7.6	0.1	0.05	1.02	0.13	0.12
8	46.45	12.5	0.1	0.18	1.51	0.06	0.03
14	46.34	17.3	0.2	0.25	1.72	0.04	0.01
20	46.24	26.6	0.2	0.29	1.82	0.03	0.01

Table 3. *Measurement results of a PiHard sample*

4.3. PiSoft sample results

The presentation of measurement results for PiSoft ceramics differs from the previous one. In this case, much more complex 3D diagrams are created from the data. In this case, the advantages of using Matlab become apparent. Different data manipulations can be easily implemented and presented to the user. In figure Fig. 19, an impedance magnitude is plotted for all measured temperatures and excitation levels. The right horizontal axis shows the measured voltage, the left horizontal axis shows the excitation frequency, and the vertical axis shows the impedance magnitude. It is important to note that the frequency scale increases from right to left as the centre of the system is rotated in this way.

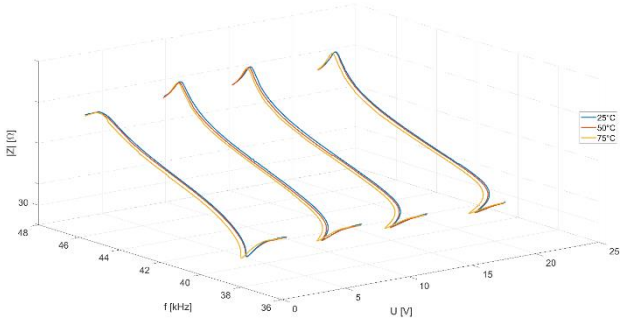

Fig.19. *Impedance magnitude of a PiSoft sample for all measured temperatures and excitations*

Numerical representation of results can be viewed in a Table 4:

U_{Exc} [V]	f_s [kHz]	|Z| [Ω]	p [mPa]	x [µm]	U_R [V]	I_R [A]	P_R [W]
2	38.76	35.2	0.1	0.04	1.63	0.05	0.08
8	38.36	53.1	0.2	0.09	1.77	0.03	0.02
14	38.11	64.0	0.2	0.12	1.86	0.02	0.01
20	37.80	74.1	0.3	0.15	1.91	0.02	0.01
2	38.81	34.3	0.0	0.04	1.67	0.05	0.08
8	38.36	50.5	0.1	0.09	1.77	0.03	0.02
14	38.16	60.8	0.2	0.12	1.85	0.02	0.01
20	37.80	71.1	0.2	0.16	1.92	0.02	0.01
2	38.96	30.1	0.0	0.04	1.54	0.05	0.08
8	38.56	47.2	0.0	0.09	1.72	0.03	0.02
14	38.26	57.2	0.1	0.12	1.82	0.02	0.01
20	37.95	66.1	0.1	0.16	1.88	0.02	0.01

Table 4. *Measurement results of a PiSoft sample*

4.4. Pi700 sample results

The last results presented are from a lead-free sample. This type of ceramics currently the subject of much research. The absence of lead (Pb) in a composite ceramic leads to a weaker piezoelectric property of the samples. Fig. 20 shows the 3D results of the impedance magnitude and Fig. 21 the pressure

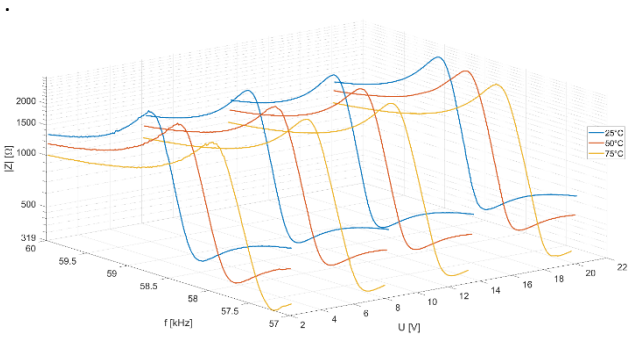

Fig.20. *Impedance magnitude of a Pi700 sample for all measured temperatures and excitations*

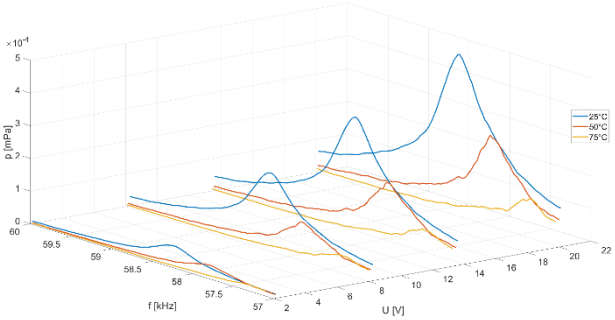

Fig.21. *Pressure results of a Pi700 sample for all measured temperatures and excitations*

U_{Exc} [V]	f_s [kHz]	|Z| [Ω]	p [mPa]	x [µm]	U_R [V]	I_R [A]	P_R [W]
2	58.13	454.2	0.1	0.02	2.08	4.57	0.01
8	58.13	460.1	0.2	0.04	2.08	4.57	0.01
14	58.12	461.6	0.4	0.06	2.08	4.57	0.01
20	58.09	461.4	0.5	0.08	2.08	4.54	0.01
2	57.68	391.7	0.0	0.02	2.05	5.24	0.01
8	57.71	394.7	0.1	0.04	2.05	5.23	0.01
14	57.69	397.6	0.2	0.06	2.05	5.24	0.01
20	57.68	404.2	0.3	0.08	2.05	5.24	0.01
2	57.21	318.8	0.0	0.02	2.02	6.33	0.01
8	57.24	327.3	0.1	0.04	2.02	6.29	0.01
14	57.23	329.2	0.1	0.06	2.02	6.31	0.01
20	57.23	333.7	0.1	0.09	2.02	6.31	0.01

Table 5. *Measurement results of a Pi700 sample*

As can be seen in Fig. 20, the magnitude of the impedance is relatively high compared to the impedance of an amplifier (50 Ω), so the measured voltage (and power) across a sample is small. Table 5 shows the results for the lead-free sample, which confirm a forementioned.

5. DISCUSSION

Performing measurements on different piezoceramic samples allows a comparison of the results, focusing on the differences between the measured ceramics. All measurements were performed in radial vibration mode, with the sample free in air, without any load.

The measurement results show that the resonant frequency of two samples (APC50 and PiHard) of the same type (hard) from different manufacturers is almost the same. There are small differences between the parameters of the hard samples, but the tendency is the same. This behaviour is as expected since both samples are hard samples with the same dimensions. From the measurements, it is easy to conclude that pressure and displacement are directly correlated with the magnitude of the impedance in this measurement setup. At the same excitation level, the highest pressure and displacement are recorded for the APC50 sample, followed by another hard piezoceramic, PiHard, then PiSoft, and the lowest measurements for the lead-free Pi700 sample. The serial resonant frequency is lower for the soft samples with the same dimensions, but it is more difficult to draw conclusions for the lead-free ceramic because the dimensions do not match. The collected data correspond to the manufacturer's data sheets of the measured samples.

It is obvious that the slope of an impedance magnitude around the resonance point is steeper for hard ceramics than for soft and even steeper compared to a lead-free samples. This slope depends on the materials dopped in a composite during the fabrication process. Ceramics with a steeply sloping impedance curve are most commonly used to convert electrical energy to mechanical energy (as transmitters) because they have a higher efficiency at a given frequency point. On the other hand, ceramics with a flatter peak of the impedance curve are used as receivers that convert mechanical energy to electrical.

The temperature of a measured sample may exceed 150 °C during measurements, which may cause damage to the temperature measuring device. To avoid potential fire hazard and other disturbances in laboratory equipment for such high temperature measurements, temperature monitoring is excluded.

From the perspective of a modern instrument designer, it is difficult to develop an excitation for an ultrasonic system. The major obstacle is the variable impedance of a piezoceramic transducer as a function of excitation strength, pressure, temperature, etc. Normally, the excitation of the ultrasonic system is an electrical circuit with constant output impedance. When connected to a piezoelectric ultrasonic transducer with variable impedance, an impedance mismatch occurs, resulting in heat dissipation and lower efficiency. This phenomenon (impedance mismatch) can be observed in Fig. 15 as a voltage drop during a measurement. The voltage drop can be given as in equation 6:

$$U_L = \left| U_{Exc} \cdot \frac{Z_L}{Z_{Exc} + Z_L} \right| \tag{6}$$

U_L and Z_L are voltage and impedance of a piezoceramic, U_{Exc} and Z_{Exc} are voltage and impedance of an excitation system. To satisfy the well-known Thevenin theorem concerning maximum energy transfer from the generator to a transducer, the output impedance of the excitation should be complex conjugate to the impedance of the piezoceramic. As a solution, the impedance of the excitation circuit can be adjusted so that the change of the ceramic impedance during the excitation can be neglected in the near-resonant field (the impedance magnitude of an excitation should be very high or very low).

6. CONCLUSION

An obvious limitation of this type of characterization is that only the piezo-active part of a transducer is considered in the characterization of ceramics. There is also an influence of the backing, the front layer, the housing, the electrical wireing and the connector. To fully characterise the transducer, all of the above factors must be considered. The data presented here is the result of measuring bulk ceramics, not assembled transducers. These results are relevant and applicable to the modelling and design of a transducer. It is easier to measure the influence of a particular component than to characterise an assembled transducer.

The data presented in this article can be implemented in the modern ultrasound systems to perform continuous excitation in resonance. As illustrated, an ultrasound transducer changes its characteristics (resonant

frequency, impedance magnitude, etc.) during excitation. In order to keep the excitation of an ultrasound transducer constantly in resonance, a frequency adaptive circuit must be developed. Although the described laboratory setup simultaneously measures the signals needed to maintain constant excitation at resonance, the frequency of refreshing the data is not satisfactory for commercial use. Furthermore, the weight and size of the equipment represents another challenge. As an answer, a self-controlling circuit must be developed using fast processing units such as DSP or FPGAs. Nowadays, a solution using a microcontroller can also be achieved, minimizing power consumption and weight.

7. ACKNOWLEDGEMENT

The results presented in this paper has been partly funded by Croatian Science Foundation under project called “Ultrasound System for Complex Material Parameters Determination in Nonlinear Working Conditions (ULTRASNON)” (project number 4996) and partly by the project “An ultrasonic non-destructive testing system for detection and quantification of early stage subsurface creep damage in the thermal power generation industry (CreepUT)” (Project ID: 760232) funded by European Union from the programme “H2020-EU.2. - PRIORITY 'Industrial leadership'” and programme “H2020-EU.3. - PRIORITY 'Societal challenges'“.

8. REFERENCES

[1.] Jaffe, B., Cook Jr., W. R., Jaffe, H.: **Piezoelectric ceramics**, *Academic Press*, London & New York, 1971

[2.] Ballato, A.: **Piezoelectricity: Old Effect, New Thrusts**, *IEEE Transactions on Ultrasonics, Ferroelectrics, and Frequency Control*, 5(42), 1995

[3.] Mason, W. P.: **Piezoelectricity, its history and applications**, *Journal of Acoustical Society of America*, 6(70), 1981

[4.] Mason, W. P.: **Piezoelectric Crystals and Their Application in Ultrasonics**, *D. Van Nostrand Company, Inc*, 1950

[5.] Kino, G. S.: **Acoustic waves, devices imaging and analog signal processing**, *Prentice-Hall Inc.*, 1987

[6.] Kuang, Y., Jin, Y., Cochran, S., Huang, Z.: **Resonance tracking and vibration stablilization for high power ultrasonic transducers**, *Ultrasonics*, 54, 2014, 187–194

[7.] **IEEE Standard on piezoelectricity, IEEE Std 176-1978**, *The Institute of Electrical and Electronics Engineers*, New York, 1978

[8.] Svilainis, L., Motiejunas. G.: **Power amplifier for ultrasonic transducer excitation,** *NDT.net,* 10, 2006

[9.] Krimholtz, R., Leedom, D. A., Matthaei, G. L.: **New Equivalent Circuit for Elementary Piezoelectric Transducers**, *Electron Letters*, 6, 1970, 398-399

[10.] Sherrit, S., Leary, S. P., Dolgin, B. P., Bar-Cohen, Y.: **Comparison of the Mason and KLM Equivalent Circuits for Piezoelectric Resonators in the Thickness Mode,** *IEEE Ultrasonics Symposium*, 1999

[11.] Castilloa, M., Acevedob, P., Moreno, E.: **KLM model for lossy piezoelectric transducers**, *ULTRASONICS*, 41, 2003

[12.] Bigelow, T. A.: **Experimental evaluation of nonlinear indices for ultrasound transducer characterizations appendix B: The KLM model**, *Master of Science Thesis*, 1998

[13.] Petošić, A., Ivančević, B., Jambrošić, K.: **Experimental and Theoretical Considerations of Ultrasound Transducers Working in Nonlinear Regime**, *Proceedings 3rd Congress of the Alps Adria Acoustics Association*, Graz, 2007, 1-10